FEDERAL UNIVERSITY OF TECHNOLOGY, AKURE
JOURNAL OF ENGINEERING AND ENGINEERING TECHNOLOGY

IN VITRO STUDY OF DIFFERENT SAMPLES OF 316 STAINLESS STEEL AS ORTHOPAEDIC BIOCOMPATIBLE MATERIALS

[1]Emoekpere, M.*, [2]Adetunji, O.R., [1]Owoeye, F. T., [1]Koya, A.K. and [3]Adewale, S. T.

[1]Department of Metallurgical Engineering, Yaba College of Technology, Lagos.

[2]Department of Mechanical Engineering, Federal University of Agriculture, Abeokuta.

[3]Department of Welding & Fabrication Engineering, Yaba College of Technology, Lagos.

**Corresponding author: michael.emoekpere@yabatech.edu.ng*

Emoekpere, M., Adetunji, O.R., Owoeye, F. T., Koya, A.K., Adewale, S. T. (2026): In vitro study of different samples of 316 stainless steel as orthopaedic biocompatible materials. FUTA Journal of Engineering and Engineering Technology 20(1), 82-90

Received Date: 21.03.2026 **Accepted Date: 01.05.2026**

Abstract

There have been constant researches in the orthopaedic field because of the necessity for improved implants to reduce complications and system damage in host tissues. This study examines the *in vitro* behaviour of different prepared samples of 316 stainless steel materials as biocompatible materials for orthopaedic applications. In this research, three samples of 316 stainless steel (SS) were prepared for *in vitro* assessments. Sample 1 was a 316SS alloy, sample 2 was heat-treated 316SS, and sample 3 was heat-treated 316SS coated with graphene. Ringer solution was prepared as the simulated body fluid (SBF) using standard reagents, and the samples were preserved in the SBF for ten (10) weeks in a water bath at 37 °C. An electrochemical test was done using the potentiodynamic polarization method (PDP). Biological assays were carried out to determine turbidity and colony-forming units (CFUs) after 60 days of culturing using McFarland standard test. The PDP showed that sample 3 had the best corrosion resistance with the highest negative corrosion potential (Ecorr) of -0.3940 (V). It also produced the most turbidity among the three samples, which were 5.7, 3.6, and 2.2, and CFUs of 2.8 x 10^8, 3.3 x 10^8 and 4.4 x 10^8 cells/mL, respectively, after 40, 50, and 60 days. The results obtained indicated that graphene coatings can lower the corrosion rate of 316 stainless steel samples and also have the ability to enhance the proliferation of organisms compared to the other prepared uncoated samples.

Keywords: biocompatible, orthopaedic, corrosion, colony-forming units, turbidity.

Introduction

A biocompatible material refers to a material that has the capacity to coexist within a biological environment, either synthetically or naturally, without compromising tissue, organ, or the general functional cohesion when employed in various systems (Gibbs, 2020; Fuentes *et al.*, 2019). These devices are employed to guide, augment, or serve as substitutes for the physiological functions of human body tissues (Gururaj and Dinesh, 2018). Biologically engineered materials and substances have been designed to interact with and regulate biological processes to achieve the medical objectives, which include therapeutic or other special applications (Kam, 1980). A primary challenge encountered in the application of biocompatible materials pertains to immune rejection, as current implant and bone replacement technologies necessitate that the materials exhibit properties consistent with the living tissues. It should also be consistent based on their biological and mechanical properties of the utilized material (Bharadwaj, 2021).

In the last century, significant advancements in metallic engineering have led to the creation of biocompatible alloys; a major example is stainless steel, which led to the development of metallic implants for osseous fixation. These materials have been further developed into various implantable devices, including screws, pins, and plates (Im, 2020). 316 stainless steel is a major stainless-steel material used as an orthopaedic implant material. This is because it exhibits satisfactory mechanical properties; however, its utilization is compromised by susceptibility to environmental corrosion in body fluids. Specifically, 316 implants experience pitting corrosion, necessitating device removal in certain instances. This phenomenon occurs primarily in oxygen-deficient regions and crevices, resulting in potential implant failure. A further limitation of 316 stainless steel in biomedical applications is its inability to consistently integrate

with surrounding tissues due to limited blood compatibility, precipitated by nickel content. In an effort to mitigate these issues, the implementation of bioactive coatings on 316 stainless steel has been explored. These coatings aim to facilitate initial organic fixation, reduce corrosion, and make up for surgical inaccuracies by enhancing device stability (Esmaeili *et al.,* 2021).

Graphene consists of a single, two-dimensional layer of sp^2-hybridized carbon atoms covalently arranged in a hexagonal lattice. It has garnered significant scientific attention due to its outstanding physical properties (Ricci *et al.*, 2022). Graphene exhibits high structural stability and inherent hydrophobicity (Destiarti *et al.*, 2021). Research indicates that graphene-based nanocoatings exhibit antiadhesive properties and facilitate enhanced bone formation on metallic biomaterials (Rosa *et al.*, 2021). Graphene and its derivative, graphene oxide, exhibit advantageous biomechanical characteristics, making them promising candidates for functional biomaterials (Triawan *et al.*, 2022). Graphene nanocoatings retain exceptional structural integrity when subjected to various stresses prevalent in the oral environment, associated with revealing minimal inflammatory responses by macrophages *in vivo*. These attributes facilitate accelerated osseointegration and reduced susceptibility to biofilm-related diseases on dental implants in living organisms (Rosa *et al.*, 2021). On investigating the biological interactions of graphene, Fadeel *et al*. reported that extensive *in vitro* (cell-based) studies conducted under the Graphene Flagship initiative demonstrated that graphene-based materials (GBMs) exhibit no cytotoxic effects on human immune cells, including macrophages, neutrophils, dendritic cells, among others (Fadeel *et al.*, 2025). However, this does not imply that these materials are entirely innocuous, as they may still modulate cellular function in the absence of evident cytotoxicity. Therefore, further investigations to assess functional responses and related cellular activities was recommended (Peng *et al.*, 2022; Fadeel *et al.*, 2025). Notwithstanding, the available evidence indicates that graphene-based materials (GBMs) do not induce significant toxicity in either *in vitro* or *in vivo* systems. However, it should be noted that GBMs are not a homogeneous class of materials, and further investigations are needed, particularly regarding other post-graphene materials (Fadeel *et al.*, 2025). With respect to biomedical applications, both graphene oxide (GO) and reduced graphene oxide (rGO) have been shown to significantly influence the proliferation and differentiation of seeded stem cells when incorporated into three-dimensional scaffolds for bone, cardiac, neural, skin, and adipose tissue regeneration (Maleki *et al.*, 2020; Ricci *et al.*, 2022). Ricci *et al.* reported a study demonstrating that GO–cellulose nanocomposites exhibit good compatibility with endothelial cells (ECs) and enhance endothelial cell migration *in vitro*, as well as promote rat skin wound healing *in vivo*, thereby facilitating neovascularization and re-epithelialization (Ricci *et al.*, 2022; Soliman *et al.*, 2021). The potential risks associated with graphene materials remain under debate, as carbon-based materials are widely encountered in everyday applications and are generally considered safe. (Destiarti *et al.*, 2021). The perception that graphene poses minimal risk is based on its low toxicity, its use in relatively small quantities, and its structural similarity to benign carbon-based materials. However, some researchers argue that graphene may present potential risks under certain conditions, particularly where existing information on its safety profile is insufficient (Destiarti *et al.*, 2021). An increase in graphene exposure concentration may be associated with a reduction in neurotransmitter levels (Destiarti *et al.*, 2021). More recently, the properties of graphene oxide (GO) have been effectively utilized in cartilage regeneration, yielding encouraging *in vitro* outcomes. Notably, graphene-based materials are increasingly recognized for their ability to modulate inflammatory pathways in immune cells, thereby enhancing and accelerating tissue regeneration following implantation (Ricci *et al*., 2022).

The composition of bones and teeth can be characterized by the presence of mineral and tissue elements, comprising cellular and matrix constituents, as well as fatty substances, polysaccharides, and polyphosphates. Bone tissue primarily comprises a mineral component, accounting for approximately 69% of its total weight, also having 9% water and 22% organic matrix content. In particular, it is primarily made up of collagen, with a range of 90-96% (Eric and Rivera-Muñoz, 2011). Hydroxyapatite (HAp), characterized by the chemical formula $Ca_{10}(PO_4)_6(OH)_2$, plays a pivotal role in this composition. The bone contains other notable calcium phosphate phases and various amorphous calcium phosphate species. Furthermore, trace amounts of impurities, comprising magnesium, sodium, chlorine, and iron, have also been detected in bone mineralisation (Eric and Rivera-Muñoz, 2011).

One major challenge with prosthetic biomaterials has been biocompatibility. Additionally, metallic biomaterials experience corrosion and other challenges that lead to removal and replacement. Several studies are being done in the area of improving the biocompatibility of implants. This work is further research into the aspect of biocompatibility of prosthetic materials. While heat treatment of metallic prosthetic materials is not a common practice, graphene has been viewed as deleterious to the human body. This research dealt

with the impact of heat treatment and graphene coating on 316 stainless steel as implant biocompatible materials in simulated body conditions.

Table 1: Reagents for preparing ringer solution as simulated body fluid (SBF)

S/N	Reagent	Amount (g/L)
1	Sodium chloride – NaCl	7.996
2	Sodium bicarbonate – $NaHCO_3$	0.35
3	Potassium Chloride – KCl	0.224
4.	Potassium phosphate dibasic trihydrate – $K_2HPO_4.3H_2O$	0.228
5	Magnesium Chloride hexahydrate – $MgCl_2.6H_2O$	0.305
6.	1 M Hydrochloric Acid – HCl	40mL
7	Calcium chloride – $CaCl_2$	0.278
8.	Sodium Sulphate – Na_2SO_4	0.071
9.	TRIS (hydroxymethyl) aminomethane – $(HOCH_2)_3CNH_3$	6.057

(Kokubo *et al.,* 1990)

Table 2: Concentration of ions in simulated body fluid and human blood plasma

S/N	Ion	Simulated Body Fluid (mM)	Human Blood Plasma (mM)
1	HCO^{3+}	4.2	27
2.	K^+	5	5
3	Cl^-	148.8	103
4.	Na^+	142	142
5.	Ca^{2+}	2.5	2.5
6.	Mg^{2+}	1.5	1.5
7	HPO_4^{2-}	1	1
8.	SO_4^{2-}	0.5	0.5
9.	TRIS (hydroxymethyl) aminomethane	50	50
10	Hydrochloric Acid	45	45
Properties			
11	pH	7.25	7.25

(Kokubo *et al.,* 1990)

In order to assess implant materials, two major processes are used: *in vitro* and *in vivo*. *In vitro,* which is the first stage, involves studies that are conducted outside the living organisms, while *in vivo,* which is the later stage, involves tests done inside the living organisms, either in animals or humans. One way of carrying out an *in vitro* test for prostheses is by using a simulated body fluid. In this research, a ringer solution was prepared and used as the simulated body fluid. Table 1 shows the reagents used for preparing Ringer's solution. The ringer solution has a concentration of ions that is almost the same as that of human blood plasma and was adjusted to a pH of 7.40 with a concentration of 50 mM TRIS hydroxymethyl aminomethane and 45mM HCl at 37 °C. Table 2 shows the ionic concentration of the reagent.

Methodology

316 stainless steel was used for this experiment. The stainless-steel samples were cut from a rod of the metal with a diameter of 30 mm. These were mechanically ground using emery papers and polished. Acetone was then used to degrease the samples, and deionized water was used to wash the samples. This was done in accordance with Pohrelyuk *et al.* (2013). Heat treatment process was carried out on the 316 stainless steel samples, where they were heated to 1000 °C to assess the impact of heat treatment on the samples.

The coating done on the sample was a thin coating and not a heavy coating. Also, the process used

enabled the coating to stick to the surface. Resistivity heating was used to coat the surface of the 316 stainless steel with graphene. The method used was material deposition by vacuum evaporation, using equipment known as PVD (Physical Vapour Deposition). The workable vacuum is in the region of 10^{-5}. This is necessary to avoid hydrocarbon buildups, as these buildups may lead to electrical breakdowns. A target storage area was adopted to make sure that the target is not degraded/oxidised by the atmosphere. A glove box as an enclosure was used to provide an inert environment to the target – this is achieved by pumping in argon gas. Deterioration/oxidation of targets is prevented by transferring the target, still under vacuum, from the evaporator to an evacuated storage chamber/glove box until required. This was carried out at the RDTS unit at iThemba LABS (Target Laboratory), Eerste River, Cape Town, South Africa.

Simulated body fluid (SBF) has a concentration of ions that is almost the same as that of human blood plasma and was adjusted to a pH of 7.40 with a concentration of 50 mM TRIS hydroxymethyl aminomethane and 1M hydrochloric acid at 37ºC. The 1 litre volumetric flask was cleaned with neutral detergent and distilled water, and then dried. 700 ml of distilled water was added to a one-litre polyethylene bottle and sealed. A magnetic stirrer was used to stir the water, and the reagents were gradually added in the sequence specified in Table 1, ensuring each reagent was fully dissolved before introducing the next. The pH of the solution was then adjusted to 7.40 by stirring and titrating with a 1M HCl solution. After removing the pH electrode, water was added to bring the solution up to one litre of the solution. It is placed on the magnetic stirrer for about 20 minutes so that the temperature of the solution can be sustained at 37 °C. The solution was poured into various smaller conical flasks, and the samples were placed inside. These were then transferred to a water bath set at 37 °C and kept for ten (10) weeks.

Electrochemical Tests

The electrochemical tests of 316 stainless steel were conducted using a potentiostat. The electrolyte that simulated the conditions of human body fluid was a Ringer's solution, which was prepared using laboratory-grade chemicals and distilled water. The experiment was performed at estimated body temperature at 36 °C and 38 °C while maintaining the pH of the solution at 7.4. The ringer solution was maintained between 36 °C and 38 °C throughout the period of this test. The corrosion behavior of samples was assessed via the use of a conventional three-electrode system, which consists of the stainless-steel samples as the working electrodes, a graphite rod counter electrode, and the reference electrode being a saturated calomel electrode (SCE). Potentiodynamic polarization was done at a scan rate of 1 mV/s from 250 mV below OCP to 1000 mV in the direction of the anode. The test was done in accordance with Pohrelyuk *et al* (2013).

Spectrophotometric Measurements

The spectrophotometric technique for assessing turbidity utilizes a prism or diffraction grating to produce incident light at a designated wavelength. Usually, the wavelengths for measuring the turbidity of bacteria are 480 nm (blue), 540 nm (green), 600 nm (orange), and 660 nm (red). Turbidity is measured in terms of optical density (OD) at the specified wavelength, such as OD540 for measurements at 540 nm. The density of a bacterial cell suspension is represented as absorbance or optical density, which correlates directly with the number of cells present.

Biological Assays

The work done was done to stimulate the action of the red and white blood cells, as well as the cellular interaction between the cells of the joints and that of the prosthesis. The interaction was done using a consortium of two bacteria (Gram-positive bacillus species) and Gram-negative pseudomonas species. The medium which simulates the blood is a mixture of salts – K_2PO_4 → 2.13 gth; KH_2PO_4 →1.30 gth; $MgSO_4$ →0.5g; NaCl → 1.5g; $FeSO_4$ → 0.04g; NH_4NO_3 → 0.8g; $CaCl_2$ → 0.02g. The medium was prepared and divided into conical flasks, duly labelled accordingly. The medium was sterilized by autoclaving at 121 °C for 25 to 30 minutes at 0.15 kPa. The medium in the conical flask had the substrate (or test prosthetic component piece) within it while sterilizing. Then, using test tubes with 3 ml of saline each, 0.5 McFarland's standard of the test organisms was prepared in the test tubes. Using a 0.1 ml micropipette, 0.1 ml of the test organisms was aseptically placed into the different conical flasks, which had already been labelled according to the samples. A spectrophotometer was used to measure the absorbance and turbidity for each of the samples after the fortieth, fiftieth, and sixtieth days, respectively.

Results

Potentiodynamic Polarization (PDP)

Figure 1 shows the graph of corrosion potential (E_{corr}) against the current density (I_{corr}) for 316 stainless steel, heat-treated 316 stainless steel, and the coated heat-treated 316 stainless steel, each in separate vessels of Ringer's solution. From the corrosion assessment after immersion in the simulated body fluid for ten (10) weeks, it was observed that the coated heat-treated 316 stainless steels in Ringer solution had the highest resistance to corrosion due to their highest negative corrosion

potential (Ecorr) of -0.3940(V) and current density of $3.06x10^{-7}$ (A/cm^2). The next was the uncoated heat-treated 316 stainless steel in Ringer's solution, which has a corrosion potential of -0.3650 (V) and current density of $3.11x10^{-7}$ (A/cm^2). The sample that recorded the least resistance to corrosion among them is the stainless steel in Ringer's solution, which has a corrosion potential of -0.2090 (V) and current density of $4.03x10^{-7}$(A/cm^2). Table 3 shows the Tafel fit results for three samples.

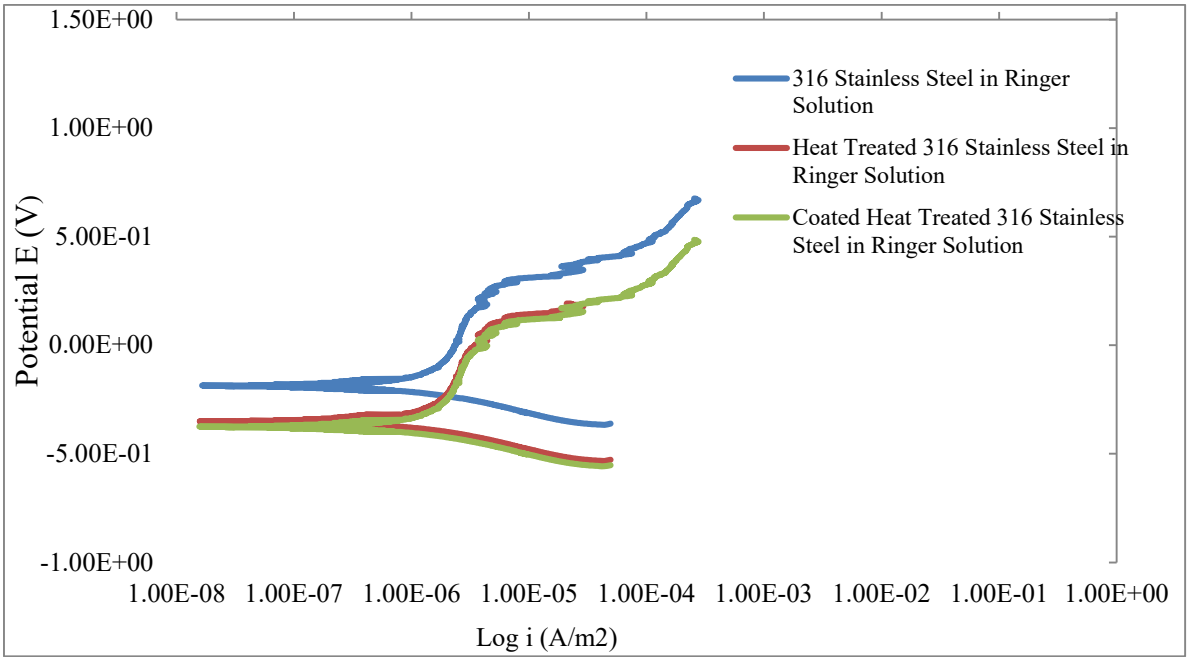

Figure 1: Potentiodynamic polarization graph of 316 SS, heat-treated 316 SS and coated heat-treated 316 SS in Ringer's solution.

Table 3: Tafel Fit Results for the PDP

Samples	Ecorr (V)	Icorr (A/cm^2)	C.R (mm/yr)	Remark on susceptibility to corrosion
316 SS in ringer	-0.2090	$4.03x10^{-7}$	$4.675x10^{-9}$	Most affected
Heat-treated 316SS in ringer	-0.3650	$3.11x10^{-7}$	$3.607x10^{-9}$	More affected
Coated heat-treated 316SS in ringer	-0.3940	$3.06x10^{-7}$	$3.55x10^{-9}$	Least affected

Table 4: Turbidity after 40 days, 50 days and 60 days

Sample	Turbidity After 40 days	Turbidity After 50 days	Turbidity After 60 days
316 SS	37.5	37.0	23.4
Heat-treated 316 SS	58.3	54.3	14.3
Coated heat-treated 316SS	5.7	3.6	2.2

Biological Assays

The optical densities of the samples were taken after the fortieth (40th), fiftieth (50th), and sixtieth (60th) days using a spectrophotometer. Table 4 shows the results of the turbidity for the samples. Turbidity reflects the density of organisms. The spectrophotometric measurements were done at OD540. The turbidity for the various samples after 40, 50, and 60 days was 5.7, 3.6, and 2.2 for the coated heat-treated 316 stainless steel sample. The uncoated heat-treated 316 stainless steel was 58.3, 54.3, and 14.3, while the 316 stainless steel had turbidity of 37.5, 37.0, and 23.4. The bar graphs of the turbidity after 40, 50, and 60 days are shown in Figure 2.

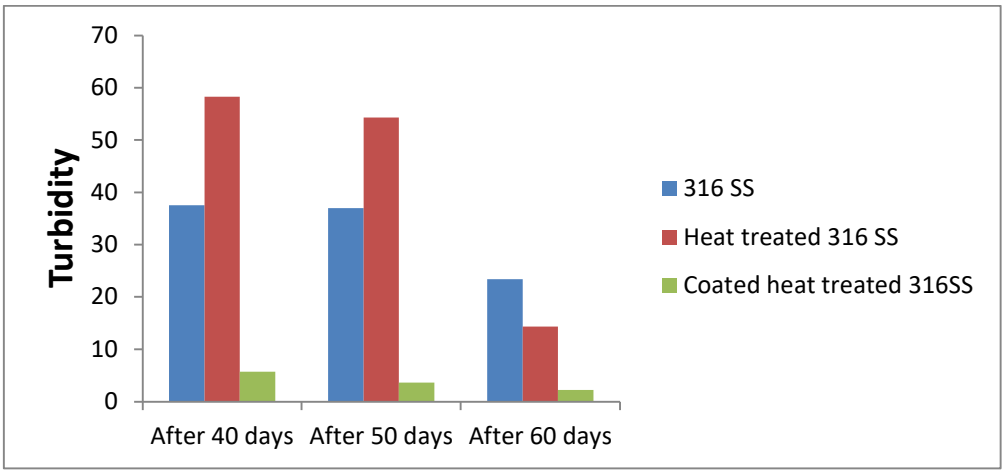

Figure 2: Turbidity of the samples after 40, 50 and 60 days, respectively.

Table 5: The CFUs of the samples after 40, 50 and 60 days respectively

	After 40 days (cells/mL)	After 50 days (cells/mL)	After 60 days (cells/mL)
316 SS	9.7×10^7	9.8×10^7	1.6×10^8
Heat treated 316 SS	5.3×10^7	5.99×10^7	1.9×10^8
Coated heat treated 316SS	2.8×10^8	3.3×10^8	4.4×10^8

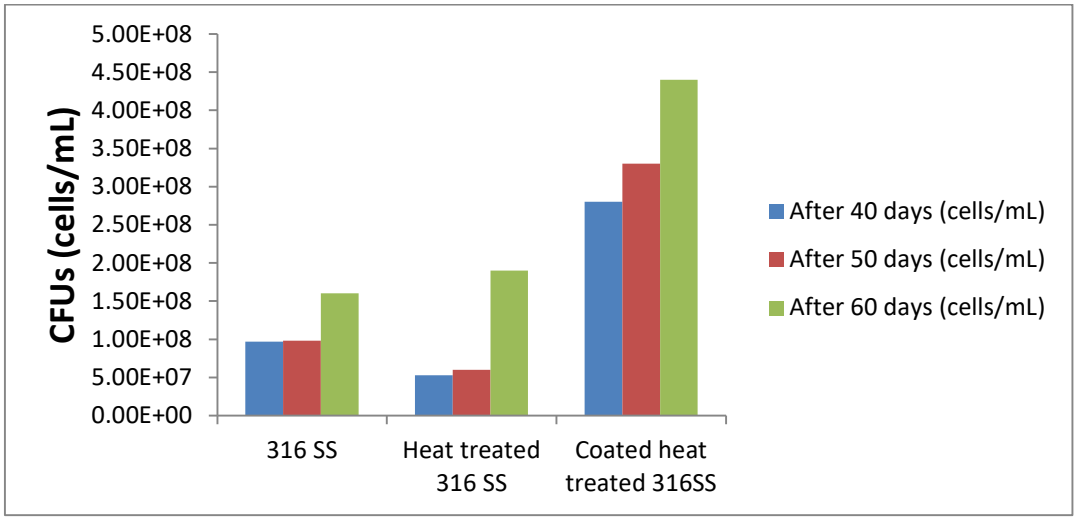

Figure 3: CFUs of the samples after 40, 50 and 60 days, respectively.

The results of the colony-forming units (CFUs) for the various samples are shown in Table 5. Here, it could be seen that the graphene-coated heat-treated 316 stainless steels had the highest organism's growth with CFUs of 2.8×10^8, 3.3×10^8 and 4.4×10^8 cells/mL, respectively, after 40, 50 and 60 days period. Also, CFUs for 316 stainless steels were 9.7×10^7, 9.8×10^7 and 1.6×10^8 cells/mL, and for heat treated 316 stainless steels were $5.3 \times 10^{7,}$ 5.99×10^7 and 1.9×10^8 cells/mL, respectively. Figure 3 shows the bar graph for the CFUs after 40, 50, and 60 days, respectively.

Discussion

For the electrochemical studies, the results showed that the heat-treated 316 stainless steels coated with graphene in Ringer's solution exhibited the highest resistance to corrosion with a corrosion potential (Ecorr) of -0.3940 (V) and current density of 3.06×10^{-7} (A/cm^2). This could be due to protective film formed on the surface of the stainless steel, which was able to passivate it from attack from the medium and hence resulted in low corrosion rate (Adetunji *et al.*, 2016). This is also confirmed by James (2022), whose research revealed that

graphene films displayed greater polarisation resistance and lower corrosion rates on SS316L. The corrosion potential obtained for the coated heat-treated 316 stainless steels in Ringer solution, which was (Ecorr) of -0.3940 (V) or -394 (mV), was lower than the results obtained and reported by Mudali *et al*. (2003), which were -373 (mV) for 316 stainless steels in Ringer solution and -108 (mV) for 316 stainless steels in Hank solutions. The next was uncoated heat-treated 316 stainless steel in Ringer's solution with corrosion potential (Ecorr) of -0.3650 (V) and current density of $3.11x10^{-7}$ (A/cm^2), while the corrosion potential (Ecorr) of the 316 stainless steel was -0.2090 (V) and current density $4.03x10^{-7}$ (A/cm^2). This showed that the heat-treated 316 stainless steels (both coated and uncoated) exhibited more corrosion resistance properties than the pure 316 stainless steel. It could be deduced that heat treatment can increase the corrosion resistance of 316 stainless steel in simulated body fluids. At temperatures between 900 °C and 1000 °C, the corrosion resistance improves due to microstructural modifications. However, at higher temperatures (above 1100 °C), the resistance may reduce due to coarsening of inclusions and formation of chromium-depleted zones (Sangoi *et al.*, 2025; Wang *et al.*, 2022).

The results for the culturing were used to assess the impact of red and white blood cells on the samples and their ability to allow faster organism proliferation. The evaluation of the samples was done after the 40th, 50th, and 60th days using a spectrophotometer. The turbidity for the various samples after 40, 50, and 60-day periods was 5.7, 3.6, and 2.2 for the coated heat-treated 316 stainless steels. It had the highest concentration of organisms and cell growth when compared to the other samples. This could be as a result of the presence of the graphene coatings, which was corroborated by Maleki *et al.* (2020) and Ricci *et al.* (2022) who reported that graphene-based materials (GBMs) have a significant influence on stem cell proliferation and differentiation when incorporated into three-dimensional scaffolds in bones. The uncoated heat-treated 316 stainless steel was 58.3, 54.3, and 14.3, while the 316 stainless steel had turbidity of 37.5, 37.0, and 23.4. For the CFUs, the highest CFU was the heat-treated 316 stainless steel coated with graphene. It had a CFU of 2.8 x 10^8, 3.3 x 10^8 and 4.4 x 10^8 cells/mL for the 40th, 50th, and 60th days, respectively. The graphene on the metal could be the reason for it having a higher CFU than the uncoated heat-treated 316 stainless steel and also better biocompatibility. This was also confirmed by Triawan *et al.* (2022), Ricci *et al.* (2022) and Soliman *et al.* (2021). Also, CFUs for 316 stainless steels were 9.7 x 10^7, 9.8 x 10^7 and 1.6 x 10^8 cells/mL and for heat-treated 316 stainless steels were 5.3 x 10^7, 5.99 x 10^7 and 1.9 x 10^8 cells/mL, respectively.

Conclusion

i. The PDP showed that the corrosion potentials for samples 1, 2 and 3 were -0.2090 (V), -0.3650 (V) and -0.3940 (V), respectively where sample 3, the graphene coated heat treated 316 stainless steels having corrosion potential (Ecorr) of -0.3940 (V) demonstrated better resistance to corrosion in the ringer solution compared to the other samples. This showed that the graphene coatings affected the materials properties of the 316 stainless steel and the corrosion resistance improved for the coated sample.
ii. Heat treatment affected the *in vitro* corrosion properties of 316 stainless steel. At an elevated temperature of 1000 °C, the corrosion resistance improved.
iii. Sample 1 had turbidity of 37.5, 37.0, and 23.4; sample 2 was 58.3, 54.3, and 14.3, and sample 3 was 5.7, 3.6, and 2.2 after the 40th, 50th, and 60th days, respectively. The CFUs for sample 1 were 9.7 x 10^7, 9.8 x $10^{7,}$ and 1.6 x 10^8 cells/mL, sample 2 was 5.3 x 10^7, 5.99 x 10^7 and 1.9 x 10^8 cells/mL, sample 3 was 2.8 x 10^8, 3.3 x 10^8 and 4.4 x 10^8 cells/mL, respectively, after 40, 50, and 60 days period. The biocompatibility and cell proliferation improved for the coated sample 3 compared to the non-coated, which also suggests that the presence of graphene encouraged proliferation and biocompatibility.
iv. Graphene, from this and previous reported research, has demonstrated various promising properties that can improve biomaterials for biomedical applications. However, it is recommended that a higher concentration of graphene should not be allowed into the body (Destiarti *et al.*, 2021), as researches are still being carried out on possible challenges of exposure to excess graphene *in vivo.*
v. Further assessment of graphene impact should be done in the area of cell function, e.g., cytokine secretion and antigen presentation.

Acknowledgement

Special thanks to Prof. Wojciech Simka of the Silesian University of Technology, Gliwice, Poland, who assisted with providing the metallic biocompatible materials and RDTS Unit at iThemba LABS (Target Laboratory), Eerste River, Cape Town, South Africa, for assisting in coating the samples with graphene.

References

Adetunji, O. R., Ude, O. O., Kuye, S. I, Dare, E.O., Alamu, K. O. and Afolalu, S. A. (2016). "Potentiodynamic Polarization of Brass, Stainless and Coated Mild Steel in 1M

Sodium Chloride Solution" *International Journal of Engineering Research in Africa*. ISSN: 1663-4144, Vol. 23, pp 1-6 Revised: 2016-03-16 doi:10.4028/www.scientific.net/JERA.23.1 © 2016 Trans Tech Publications, Switzerland

Bharadwaj, A. (2021). "An Overview on Biomaterials and Its Applications in Medical Science". *IOP Conf. Ser.: Mater. Sci. Eng.* 1116 012178.

Destiarti, L., Kartini, I., Riyanto, Roto and Mudasir (2021). "Risk analysis and solution of using graphene: Material, synthesis, and application (Mini review)" *IOP Conf. Series: Earth and Environmental Science* 926 012054 doi:10.1088/1755-1315/926/1/012054

Eric M. and Rivera-Muñoz, E. M. (2011). "Hydroxyapatite-Based Materials: Synthesis and Characterization". Published: August 1st, 2011. DOI: 10.5772/19123

Esmaeili, A., Ghaffari, S.A., Nikkhah, M., Ghaini, F.M., Farzan, F. and Mohammad, S. (2021). "Biocompatibility assessments of 316L stainless steel substrates coated by Fe-based bulk metallic glass through electro-spark deposition method". *Colloids and Surfaces B: Biointerfaces*. Volume 198, Elsevier.

Fadeel, B., Baker, J., Ballerini, L., Bussy, C., Carniel, F.C., Tretiach, M.,…. Prato, M. (2025). "Safety Assessment of Graphene-Based Materials" *Small*. Jan 15;21(7):2404570. doi: 10.1002/smll.202404570

Fuentes, E., Alves, S., López-Ortega, A., Mendizabal, L., & de Viteri, V. S. (2019). "Advanced Surface Treatments on Titanium and Titanium Alloys Focused on Electrochemical and Physical Technologies for Biomedical Applications". *Biomaterial-supported Tissue Reconstruction or Regeneration*. IntechOpen.

Gibbs, A. (2020). "Osseointegration and biocompatibility of titanium implants". URMSE Vol. 1 DOI: 10.6069/FK5M-Z302

Gururaj, H. and Dinesh, K. R., (2018). "Polymers used as implant Biomaterials: A Review" Conference Paper available at https:// www.researchgate.net/publication/330753275

Im, G. (2020). "Biomaterials in orthopaedics: the past and future with immune modulation" *Biomaterials Research* (2020) 24:7. https://doi.org/10.1186/s40824-020-0185-7

James, L. A. (2022). "Graphene Layers for Corrosion Protection of Steel". Master of Applied Science (Research), School of Chemistry and Physics, Queensland University of Technology 74pp. http://eprints.qut.edu.au

Kam W.L. (1980). "Biomaterial", Material Science, Biomedical Engineering,Columbia University (Wikipedia).Pp 1.

Kokubo, T., Kushitani, H. Sakka, S. Kitsugi, T. and Yamamuro, T. (1990). "Solutions able to reproduce in vivo surface-structure changes in bioactive glass-ceramic A-W", ***J.*** *Biomed. Mater. Res.,* 24, 721-734.

Maleki M., Zarezadeh R., Nouri M., Sadigh A.R., Pouremamali F., Asemi Z., Kafil H.S., Alemi F. and Yousefi B. (2020). "Graphene Oxide: A Promising Material for Regenerative Medicine and Tissue Engineering". *Biomol. Concepts.* 11:182–200. doi: 10.1515/bmc-2020-0017. [DOI] [PubMed] [Google Scholar]

Mudali, U. K, Sridhar, T. M. and Raj, B. (2003). "Corrosion of bio implants". *Sadhana* Vol. 28, Parts 3 & 4, June/August 2003, pp. 601–637. © Printed in India

Peng G., Keshavan S., Delogu L., Shin Y., Casiraghi C., and Fadeel B. (2022). "Two-Dimensional Transition Metal Dichalcogenides TriggerTrained Immunity in Human Macrophages through Epigenetic and Metabolic Pathways" *Small* 18, 2107816. [DOI] [PubMed] [Google Scholar]

Pohrelyuk, I.M., Fedirko, V.M., Tkachuk, O.V. and Proskurnyak, R.V. (2013). "Corrosion Resistance of Ti–6Al–4V Alloy with Nitride Coatings in Ringer's Solution". *Corrosion Science* 66:392-398 · January 2013

Ricci, A., Cataldi, A., Zara, S. and Gallorini, M. (2022). "Graphene-Oxide-Enriched Biomaterials: A Focus on Osteo and Chondroinductive Properties and Immunomodulation". Materials (Basel). Mar 17;15(6):2229. doi: 10.3390/ma15062229.

Rosa, V., Malhotra, R., Agarwalla, S.V., Morin, J.L.P., Luong-Van, E.K., Han, Y.M., Chew, R.J.J., Seneviratne, C.J., Silikas, N., Tan, K.S., Nijhuis, C.A. and Castro Neto, A.H. (2021). "Graphene Nanocoating: High Quality and Stability upon Several Stressors". *Journal of Dental Research,* Vol. 100(10) 1169–1177. DOI:10.1177/00220345211024526 journals.sagepub.com/home/jdr

Sangoi, K., Nadimi, M., Song, J. and Fu, Y. (2025).

"Heat Treatment Effect on the Corrosion Resistance of 316L Stainless Steel Produced by Laser Powder Bed Fusion". *Metals*, 15, 41. https://doi.org/10.3390/met15010041

Soliman M., Sadek A.A., Abdelhamid H.N. and Hussein K. (2021). "Graphene oxide-cellulose nano-composite accelerates skin wound healing". *Res. Vet. Sci.* 137:262–273. doi: 10.1016/j.rvsc.2021.05.013. [DOI] [PubMed] [Google Scholar]

Triawan, F., Surya, M.J., Handayani, M., and Nandiyanto, A.B.D. (2022). "Investigation of Graphene Oxide-Based Nano composite Coating Rupture Strength on Titanium Alloy by Tensile Test for Orthopaedic Implant" *Journal of Engineering Science and Technology.* Vol. 17, No. 4; 2846 – 2860; School of Engineering, Taylor's University.

Wang, K.; Chao, Q.; Annasamy, M.; Hodgson, P.D.; Thomas, S.; Birbilis, N.; Fabijanic, D. (2022). "On the pitting behaviour of laser powder bed fusion prepared 316L stainless steel upon post-processing heat treatments". *Corros. Sci.*, 197, 110060.